Solution and Solid-State Structures of Lithiated Cyclic Phosphonates

Scott E. Denmark,* Kevin A. Swiss, Paula C. Miller, and Scott R. Wilson

Roger Adams Laboratory, Department of Chemistry, University of Illinois, Urbana, Illinois, 61801

Received 18 July 1997

ABSTRACT

*Spectroscopic analysis of lithiated cyclic phosphonates belonging to the 1,3,2-dioxaphosphorinane 2-oxide class have been examined by NMR spectroscopy in THF and by single-crystal X-ray crystallography. Lithio P-benzyl-1,3,2-dioxaphosphorinane 2-oxide (Li$^+$**7**$^-$) and lithio P-isopropyl-1,3,2-dioxaphosphorinane 2-oxide (Li$^+$**8**$^-$) are characterized by freely rotating, sp²-hybridized anions devoid of lithium–carbon contacts. The anions are most likely dimers linked through oxygen-lithium bridges. The P-isopropyl compound crystallized from TMEDA/THF as a C-lithiated dimer in which each lithium bridges a carbon and an oxygen and is solvated by one TMEDA molecule.* © 1998 John Wiley & Sons, Inc. Heteroatom Chem 9:209–218, 1998

INTRODUCTION

The carbonyl olefination reaction of stabilized organophosphonate anions [Horner-Wadsworth-Emmons (HWE) reaction] is among the most powerful carbon–carbon double-bond-forming processes [1]. Nearly every type of stabilizing group has been attached to the reactive carbon, and very good geometrical control can be obtained in most di- and some trisubstituted olefins. Despite the enormous synthetic utility of the reaction, there are still limitations, most notably the variable results obtained in ketone olefination and the problem of controlling double-bond geometry in more highly substituted cases.

Our interest in studying lithiated phosphonates derives from our general program on the design, development, and application of chiral, phosphorus-based anionic reagents [2]. We have extensively investigated these features in phosphonamide [3], thiophosphonamide [4], and phosphine oxide [5] anions, and recent reports from these laboratories have disclosed the solution and X-ray structures of lithio phosphonamides Li$^+$**1**$^-$ [3a], Li$^+$**3**$^-$ [3b], and Li$^+$**5**$^-$ [3c], lithio thiophosphonamides Li$^+$**2**$^-$ [4a] and Li$^+$**4**$^-$ [4c], and lithio phosphine oxide Li$^+$**6**$^-$ [5] (Figure 1). These anions have strikingly similar characteristics: (1) none of the anions possesses a C–Li contact, (2) the benzylic moiety is antiparallel to the P=X bond, and (3) the anionic carbon is nearly planar. We now describe the solution and solid-state structure of the oxygen analogs of **1** and **3** and compare the features of the phosphonates to the phosphoramides and phosphine oxide.

BACKGROUND

The structure of metallated phosphonate anions has been spectroscopically investigated by several groups. Early work by Cotton and Schunn involved the use of IR spectroscopy to study the anions of β-keto phosphonates that were often used in the Hor-
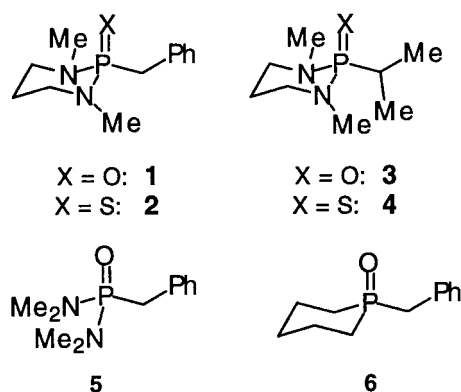
FIGURE 1 Precursors of structurally defined, lithiated phosphoryl-stabilized anions.

ner-Wadsworth-Emmons (HWE) olefination [6a]. However, a more thorough examination of the structures of β-keto phosphonate and β-cyanophosphonate anions by IR and later by X-ray crystallography was reported by Kirilov and Petrov [7]. The most comprehensive examination of the solution structure of these anions by multinuclear NMR spectroscopy is due to Seyden-Penne and coworkers [8]. This group laid the foundation for study of stabilized carbanions and contributed importantly to the understanding of geometrical control in the HWE reaction. More recently, Sauvignac [9] and Yuan [10] have reported on the structure and conformation of allyl- and benzylphosphonate anions in solution. Further, the NMR spectra of metallated benzylphosphonates have been examined by Pagini in an attempt to quantify the delocalization of charge for various benzyl anions [11]. Perhaps the most important contribution to the understanding of bonding in phosphonate anions is due to Boche and coworkers, who determined the solution and solid-state structure of the lithio dimethyl *P*-benzylphosphonate anion [12]. They found a dimer in both solid state and solution state by cryoscopy. They reported that the anion was sp^2 hybridized with a Li-O-Li-O rhombus and no lithium–carbon interaction. Additionally, some transition metal phosphonate anion complexes have been prepared and examined [13].

RESULTS AND DISCUSSION

Preparation of Substrates

The two phosphonates employed in this study were the *P*-benzyl and *P*-isopropyl-5,5-dimethyl-1,3,2-dioxaphosphorinane 2-oxides, (**7**) and (**8**), respectively. These compounds were prepared in a straightforward manner by reaction of 2,2-dimethyl-1,3-pro-

panediol with benzylphosphonic dichloride and ethylphosphonic dichloride to afford **7** directly in 54% yield and *P*-ethyl analog **9** in 83% yield. Methylation of **9** with *n*-BuLi/MeI afforded **8** in 58% yield.
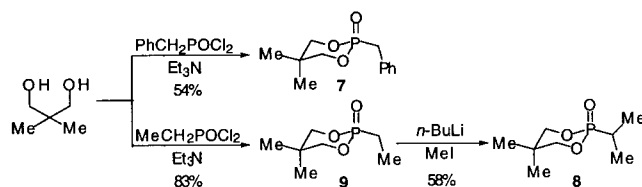
SCHEME 1

NMR Spectroscopy

For both compounds, a full set of NMR spectra was recorded in THF-d_8 at variable temperatures to establish the important changes upon metallation. The key structural features of interest are the changes in hybridization, conformation of the anionic unit, location of the lithium ion, and aggregation state. The change in transforming the neutral precursor to the lithiated compounds will be discussed to clarify the trends for both compounds.

2-Benzyl-5,5-dimethyl-1,3,2-dioxaphosphorinane 2-Oxide (**7**). In our previous studies on phosphonamides, we found that ^{13}C NMR spectroscopy provides the most useful information for clarifying anion structure and will be presented first here. Examination of **7** and Li$^+$**7**$^-$ by ^{13}C NMR spectroscopy at 20°C revealed large changes in chemical shifts (see Table 1). The most dramatic changes were seen in the phenyl substituent. For example, the ipso carbon C(7) was shifted downfield ($\Delta\delta$ = 16.8 ppm), whereas the ortho carbons C(8,12) and para carbon C(10) were shifted upfield ($\Delta\delta$ = −10.9 ppm and $\Delta\delta$ = −15.5 ppm, respectively). The carbanionic carbon C(6) was shifted slightly downfield $\Delta\delta$ = 3.1 ppm, and a significantly larger phosphorus–carbon coupling constant Δ^1J_{CP} = 95.7 Hz was found. On the other hand, the phosphorinane ring carbons changed only slightly.
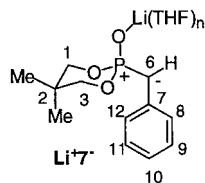
At −100°C, significant differences in the ^{13}C NMR spectrum of Li$^+$**7**$^-$ were noted. First, the slow rotation of the benzene ring caused both ortho and meta carbons to decoalesce to two resonances while several resonances were found to be unusually broadened at this temperature. Additionally, the carbon-phosphorus coupling constant of the carbanion increased to Δ^1J_{CP} = 110 Hz. The proton-carbon coupling constant for C(6) increased dramatically (Δ^1J_{CH} = 26.3 Hz) while those for the ring carbons C(1,3) decreased slightly Δ^1J_{CH} = −6.4 Hz.

Large changes were also seen in the ^{1}H NMR

spectrum at 20°C upon deprotonation (Table 2). All of the phenyl protons were shifted upfield, but as would be expected, the ortho HC(8,12) and para protons HC(10) were shifted more upfield ($\Delta\delta = -0.8$ ppm and $\Delta\delta = -1.2$ ppm, respectively) than the meta protons HC(9,11) ($\Delta\delta = -0.6$ ppm). The proton on the carbanion HC(6) was shifted upfield as well, $\Delta\delta = -1.0$ ppm. Reexamination of the anion at $-100°C$ revealed several changes. The ortho HC(8,12) and meta HC(9,11) protons decoalesce to give two sets of different resonances. One of the new ortho resonances remained broad and did not sharpen upon cooling to $-105°C$. Both sets of ring protons HC(1,3) were very broadened. The ^{1}H NMR spectra of the anion are similar to those reported for Li$^+$1$^-$ and Li$^+$5$^-$. The proton-phosphorus coupling

TABLE 1 ^{13}C NMR Data for **7** and Li$^+$**7**$^{-a}$

Me–P structure diagram with labels: Li(THF)$_n$, O, P$^+$, positions 1, 2, 3, 6, 7, 8, 9, 10, 11, 12, Me, H, Li$^+$**7**$^-$

Temp., °C	C(1,3) ($^2J_{CP}$)	C(2) ($^3J_{CP}$)	C(6) ($^1J_{CP}$)	C(7) ($^2J_{CP}$)	C(8,12) ($^3J_{CP}$)	C(9,11)	C(10)
7							
20	75.55 (d, 6.2)	33.09 (d, 7.2)	32.36 (d, 132.9)	133.30 (d, 9.6)	130.75 (d, 5.6)	128.92	127.22
−100	76.19	33.09	29.12 (d, 125.8)	133.51 (d, 7.5)	130.82 (d, 4.7)	129.05	127.16
Li$^+$7$^-$							
20	76.21 (d, 5.7)	32.84 (d, 3.3)	35.45 (d, 228.6)	150.14 (d, 13.6)	119.86 (d, 15.5)	128.07	111.74
−100	75.63	32.57	36.18 (br d, 236)	149.43 (d, 11.0)	120.80 (d, 24.1) 118.90	128.18 (br) 128.00 (br)	111.93

$^a\delta$ in ppm, J in Hz.

TABLE 2 ^{1}H NMR Data of **7** and Li$^+$**7**$^{-a}$

Temp., °C	H(1,3)$_{ax}$ ($^3J_{HP}$, J_{HH})	H(1,3)$_{eq}$ ($^3J_{HP}$, J_{HH})	H(6) ($^2J_{HP}$)	H(8) (J_{HH})	H(12) (J_{HH})	H(9) (J_{HH})	H(11) (J_{HH})	H(10) (J_{HH})
7								
20	4.05 (t, 10.7)	3.76 (dd, 12.7, 11.0)	3.21 (d, 21.5)	7.30 (m)		7.23 (t, 7.5)		7.17 (tt, 7.0, 2.2)
−100	3.88 (br dd, 19.4 10.8)	4.30 (br d, 9.6)	3.46 (d, 20.3)	7.37 (m)		7.28 (t, 7.4)		7.22 (t, 7.3)
Li$^+$7$^-$								
20	3.94 (dd, 10.4 8.7)	3.68 (dd, 16.5 10.6)	2.20 (d, 18.8)	6.52 (d, 7.9)		6.60 (t, 7.5)		5.98 (t, 7.0)
−100	3.88 (br m)		2.24 (d, 19.3)	6.76 (br)	6.26 (d, 7.7)	6.66 (t, 6.9)	6.62 (t, 7.6)	6.02 (t, 6.9)

$^a\delta$ in ppm, J in Hz.

constant for HC(6) ($^2J_{HP}$ = 19.3 Hz) shows that the anti conformer of the anion is preferred but no decoalescence was observed. In addition to the slowed rotation about the C(6)–C(7) bond, the broadening of one ortho resonance suggests that chair–chair exchange is slowing to the NMR timescale.

The ^{31}P and ^{7}Li NMR spectral data for both anions are found in Table 3. Upon deprotonation of **7** at 20°C, the ^{31}P resonance shifted downfield dramatically ($\Delta\delta$ = 21.2 ppm). After cooling to −100°C, the ^{31}P resonance of Li$^+$**7**$^-$ became extremely broad with the similar downfield shift. The ^{7}Li NMR spectrum of Li$^+$**7**$^-$ at −100°C displayed a broad resonance at δ −0.16 ppm with a width of 7.9 Hz. Remarkably, at temperatures down to −150°C, no ^{6}Li–^{31}P coupling was observed.

The spectroscopic data for Li$^+$**7**$^-$ mirrors those of the other benzylic stabilized anions Li$^+$**1**$^-$ and Li$^+$**5**$^-$. Comparison of the diagnostic features of Li$^+$**7**$^-$ and Li$^+$**1**$^-$ are compiled in Tables 4 and 5. The carbanionic carbon is clearly sp^2 hybridized as determined by the large change in $^1J_{CP}$ and $^1J_{CH}$ that has been correlated with an increase in s-character [8b]. The phenyl ring contributes significantly to charge delocalization through resonance as judged by the large upfield shifts of the ortho and para carbons and protons after deprotonation [11a]. Additionally, the C(6)–C(7) bond rotation slows to give two sets of ortho and meta resonances, as a consequence of the partial double-bond character due to extensive resonance delocalization. The phosphonyl group is polarized to stabilize the anion as evidenced by the dramatic downfield shift of the phosphorus resonance. The anion conformation O-P-C-C is predominantly anti as has been observed in the solid-state structures of Li$^+$**1**$^-$ and Li$^+$**5**$^-$ and has also been shown to be preferred computationally [4c]. Unfortunately, the aggregation state of the anion could not be determined due to the chair–chair line broadening; however, it is likely the anion exists in a similar Li-O-Li-O rhombic dimer as found for Li$^+$**1**$^-$.

2-(1-Methylethyl)-5,5-dimethyl-1,3,2-dioxaphosphorinane 2-Oxide (**8**). The spectroscopic examination of this phosphonate was complicated by poor solubility in THF at low temperature and thermal instability of the anion. Thus, we decided to make low-temperature comparisons at −80°C, where both compounds could be easily studied. The ^{13}C NMR spectrum in THF at −80°C was extremely informative (Table 6). The carbanionic carbon C(6) was shifted upfield ($\Delta\delta$ = −11.1 ppm) and a larger carbon–phosphorus coupling constant (Δ^1J_{CP} = 146.8 Hz) was observed. Interestingly, the isopropyl methyl carbons C(7,8) were shifted downfield ($\Delta\delta$ =

3.8 ppm), whereas the other resonances were only slightly changed. The isopropyl methyl carbons C(7) and C(8) showed negative hyperconjugation as determined by the downfield shift upon deprotonation and increase in $^1J_{CH}$. However, these resonances did not decoalesce upon cooling the sample to −80°C, which indicated that rapid rotation of the anion was still occurring. Indeed, from our analysis of the origin of the barrier in phosphonyl-stabilized anions, we would expect the barrier in Li$^+$**8**$^-$ to be the lowest of all [4c].

The ^{1}H NMR spectra in THF provide similar insights as for Li$^+$**7**$^-$ (Table 7). For example, the ring protons H(1,3) were shifted upfield ($\Delta\delta$ = −0.1 and $\Delta\delta$ = −0.45 ppm), whereas the isopropyl methyl protons H(7,8) were shifted downfield ($\Delta\delta$ = 0.4 ppm). In the ^{31}P NMR spectrum of Li$^+$**8**$^-$, the phosphorus resonance was shifted downfield ($\Delta\delta$ = 5.6 ppm) at −80°C (Table 3). The ^{7}Li NMR spectrum at −100°C displayed a single resonance at δ −0.61 of moderate linewidth. Finally, we were able to observe a triplet in the ^{6}Li NMR spectrum at −100°C with $^2J^6_{LiP}$ = 1.1 Hz (Table 4).

As in the case of Li$^+$**3**$^-$, a large increase in Δ^1J_{CP} is observed, indicating an sp^2 hybridized anion (Table 5). Additionally, the C(6) is shifted significantly upfield as would be expected for an sp^2 anion bearing partial negative charge. The phosphonyl group stabilizes the anion by a dipolar process, since the phosphorus is again shifted downfield. From the observed lithium–phosphorus coupling, we could discern that the anion is dimeric, most likely with a Li-O-Li-O rhombus as was shown crystallographically for Li$^+$**3**$^-$.

In view of the surprising results from the X-ray crystallographic analysis of Li$^+$**8**$^-$ (vide infra), we also examined this anion in TMEDA solution. Spectroscopic analysis in this solvent presented several problems, however, including the narrow dynamic range of the TMEDA, multiple aggregates, and high freezing point of TMEDA (−55°C). Some investigations were performed in mixtures of tetramethylpropanediamine and TMEDA to lower the freezing point of the solvent. To facilitate the analysis of the spectra, we employed isotopically enriched [^{13}C(6)] material and examined the anions at −25°C. In pure TMEDA, the ^{13}C NMR spectrum displayed an upfield shift of C(6) ($\Delta\delta$ = −15.4 ppm) and a modest increase in the one-bond coupling (Δ^1J_{CP} = 63.5 Hz). However, in a mixture of 3/1-tetramethylpropanediamine/TMEDA, the carbanionic carbon was shifted further upfield, and the carbon–phosphorus coupling constant was found to decrease with decreasing temperature. At −100°C, the one-bond carbon–

TABLE 3 ^{31}P, ^{7}Li NMR Data of Li$^+$**7**$^-$ and Li$^+$**8**$^{-a}$

		7	Li$^+$7$^-$		8	Li$^+$8$^-$	
Nucleus	Temp., °C	δ	δ	$W_{1/2}$, Hz	δ	δ	$W_{1/2}$, Hz
^{7}Li	20		0.08	5.3			
^{7}Li	−100		−0.16	7.9		−0.61	9.0
^{31}P	20	20.36	41.60		31.41	39.38	
^{31}P	−100	20.37	40.13 br		31.21^b	36.83^b	

$^a\delta$ in ppm, J in Hz.
^{b}Temp. −80°C.

TABLE 4 Selected Aggregation Data for Li$^+$**7**$^-$ and Li$^+$**8**$^{-a}$

Compound	$\Delta\delta$ ^{31}P NMR at −100°C	^{7}Li NMR at −100°C	^{6}Li NMR ($^2J_{6LiP}$)
Li$^+$7$^-$	19.7	−0.16^c	n/a
Li$^+$1$^-$	16.1	−0.06	(t, 1.0)
Li$^+$8^{-b}	5.0	−0.61	(t, 1.1)
Li$^+$3$^-$	8.0	−0.41	(t, 1.0)

$^a\delta$ in ppm, J in Hz.
^{b}At −80°C.
^{c}Resonance is extremely broad.

TABLE 5 Selected Hybridization Data for Li$^+$**7**$^-$ and Li$^+$**8**$^{-a}$

Compound	Temp., °C	$\Delta^1J_{CH}{}^a$	$\Delta^1J_{CP}{}^a$	$\Delta\delta$ ^{13}C NMR C(6)^b
Li$^+$7$^-$	20	26.3	95.7	3.1
Li$^+$1$^-$	20	26.5	103.8	4.4
Li$^+$8^{-b}	−20	n/a	129.3	−14.2
Li$^+$8^{-c}	−25	n/a	63.5	−15.4
Li$^+$3$^-$	20	n/a	102.8	−19.8

$^a\delta$ in ppm, J in Hz.
$^b\delta$(anion) − δ(neutral).
^{c}In THF solution.
^{d}In TMEDA solution.

phosphorus coupling constant of $^1J_{CP} = 178.2$ Hz was observed.

Taken together, these data imply the presence of either a rapidly equilibrating mixture of sp^3 and sp^2 anions or an intermediate hybrid in the TMEDA and 3/1-tetramethylpropanediamine/TMEDA solvents since the s-character indicator, $^1J_{CP}$, is in an intermediate range between sp^2 and sp^3. At lower temperature, the sp^3 anion predominates as indicated by the smaller one-bond carbon–phosphorus coupling constant. This implies that the amine solvents are less capable of solvating the lithium compared to THF, and the cation finds its greatest stabilization by association at the carbanionic center.

X-ray Crystallography

Although we were unable to induce crystallization of either of the anions from THF solutions, it was pos-

TABLE 6 ^{13}C NMR Data for **8** and Li$^+$**8**$^{-a}$

Li$^+$8$^-$

Temp., °C	C(1,3) ($^2J_{CP}$)	C(2) ($^3J_{CP}$)	C(4)	C(5)	C(6) ($^1J_{CP}$)	C(7,8) ($^2J_{CP}$)
8 −80	74.54 (d, 4.8)	33.34	21.20		22.42 (d, 136.2)	16.09 (br)
Li$^+$8$^-$ −80	75.51 (d, 9.0)	31.27 (d, 2.3)	22.24	21.42	11.34 (d, 283.0)	19.90 (d, 19.5)

$^a\delta$ in ppm, J in Hz.
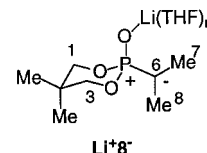
sible to generate X-ray quality crystals of Li$^+$**8**$^-$ from TMEDA containing 5% THF. The crystal and experimental data for Li$^+$**8**$^-$ are compiled in Table 8 and an ORTEP projection is found in Figure 2. Unlike any of the anions from substrates shown in Figure 1, the solid-state structure of Li$^+$**8**$^-$ reveals a carbon–lithium contact in a TMEDA solvated dimer [14]. The two monomeric units are related by an inversion center, and the core of the structure constitutes an eight-membered ring with a repeating O-P-C-Li unit. A selection of structural features is collected in Table 9. The C–Li distance is 2.228 Å, clearly indicating a strong contact between these atoms. Consequently, the carbanion is highly pyramidalized (Σ_{angles} C(1) = 347.4°). The P(1)–C(1) bond is significantly shortened (1.681 Å) compared to neutral phosphonates (ca. 1.80 Å) and is similar in length to that of the other lithiated anions without C–Li contacts.

Why does Li$^+$**8**$^-$ bridge through both carbon and oxygen whereas all of the other anions bridge through oxygen alone? Other than the imponderable issue of relative solubility of various species, we propose that the answer involves a combination of two
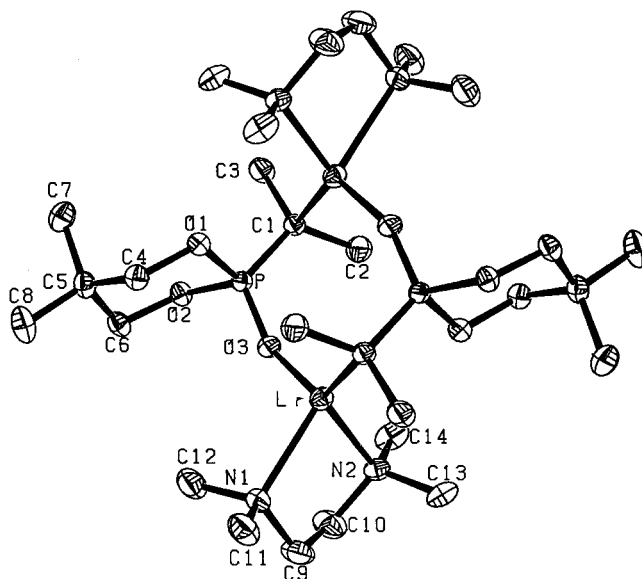
TABLE 7   ¹H NMR Data of **8** and Li⁺**8**⁻ ᵃ

Temp., °C	H(1,3)ₐₓ (J_{HH})	H(1,3)ₑq (J_{HH})	H(4)	H(5)	H(6) (J_{HH})	H(7) (J_{HH})	H(8) (J_{HH})
8							
−80	4.09 (t, 10.2)	3.87 (t, 11.6)	1.05 (s)	0.99 (s)	2.18 (m)	1.14 (dd, 17.9, 7.1)	
Li⁺**8**⁻							
−80	4.00 (d, 9.6)	3.42 (dd, 20.0, 9.7)	1.16 (s)	0.71 (s)	n/a	1.56 (d, 15.5)	

ᵃ δ in ppm, *J* in Hz.

TABLE 8   Crystal and Experimental Data for Li⁺**8**⁻

Crystal system	triclinic
Space group	P-1
a, Å	8.488(2)
b, Å	11.350(3)
c, Å	11.360(3)
α, deg.	60.81(2)
β, deg.	83.52(2)
γ, deg.	74.88(2)
V Å³	922.2(4)
Z	2
ρ (calcd) g/cm³	1.132
Temperature (°C)	−75
Dimensions	0.3 × 0.4 × 0.4
Color, habit	colorless transparent equidimentional
μ, mm-1	0.153
Absorption correction	0.961 − 0.946
2Θ limit deg. (octants)	52.0 (± *h* ± *k* + *l*)
Intensities measd (unique)	5228 (3617)
Intensities > 2.58σ(I)	2481
R	0.042
R_w (p)	0.056 (0.03)
Final difference Fourier, e/Å³	+0.24 to −0.23

FIGURE 2   ORTEP representation (35% thermal ellipsoids) of the dimer unit of Li⁺**3**⁻.

important factors: (1) the accessibility of the carbanionic carbon and (2) the steric bulk of TMEDA [15]. Our previous studies on the solution structure of thiophosphonamide-stabilized anions showed clearly that the propensity for carbon–lithium interaction is related to the steric encumbrance of the carbanion. While this is a tertiary carbanion, the lack of ring substituents in the 1 and 3 positions makes the carbon accessible to the lithium cation. Further, the greater steric bulk of TMEDA compared to THF prevents the anion from dimerizing in the usual four-membered rhomboid motif. This would require the two lithium atoms to bring the two attendant TMEDA molecules uncomfortably close and create serious nonbonded interactions. The importance of the solvation effect is clearly seen in the difference in the carbanion hybridization in THF and

TMEDA. These observations have obvious significance in the understanding of differential chemical reactivity of such metallated species in different solvents.

CONCLUSION

The lithiated cyclic phosphonates examined herein were found to be structurally similar to the *P*-benzyl and *P*-isopropyl phosphonamides and thiophosphonamides described previously. The lithium–oxygen affinity dominates the bonding, giving rise to freely rotating anions devoid of lithium–carbon contacts in THF. The *P*-isopropyl anion takes on a different structure in TMEDA with a lesser hybridization change and was crystallized from TMEDA as a *C*-lithiated dimer. The structural variability of lithiated phosphoryl compounds further illustrates the wealth of opportunities for diverse synthetic reagents and simultaneously provides a caution to the

TABLE 9 Selected Bond Lengths, Bond Angles, and Torsional Angles for Li$^+$**8**$^-$

Bond Lengths, Å

P(1)-O(3)	1.486(2)	Li(1)-O(3)	1.860(4)	C(1)-Li(1)^a	2.228(5)
P(1)-O(1)	1.619(2)	Li(1)-N(1)	2.378(5)	C(1)-C(2)	1.514(4)
P(1)-O(2)	1.621(2)	Li(1)-N(2)	2.165(4)	C(1)-C(3)	1.514(4)
P(1)-C(1)	1.681(3)				

Bond Angles, (°)

O(3)-P(1)-C(1)	119.5(1)	O(1)-P(1)-O(2)	99.48(9)
O(3)-P(1)-O(1)	109.81(10)	P(1)-O(3)-Li(1)	150.7(2)
O(3)-P(1)-O(2)	109.61(9)	P(1)-C(1)-Li(1)^a	101.2(2)
P(1)-C(1)-C(2)	117.7(2)	N(1)-Li(1)-N(2)	81.7(2)
P(1)-C(1)-C(3)	115.4(2)	N(1)-Li(1)-C(1)^a	108.9(2)
O(3)-Li(1)-N(1)	107.5(2)	O(3)-Li(1)-N(2)	106.0(2)

Torsional Angles, (°)

O(1)-P(1)-C(1)-C(2)	149.7(2)	O(1)-P(1)-C(1)-C(3)	−70.6(2)
P(1)-O(3)-Li(1)-C(1)^a	11.0(5)	O(1)-P(1)-C(1)-Li(1)^a	43.6(2)

^{a}At equivalent position ($-w, -y, -z$).

overly simplistic depiction of these most common species.

EXPERIMENTAL

^{1}H NMR and ^{13}C NMR spectra were recorded at 300 MHz ^{1}H (75.5 MHz ^{13}C, 121.4 MHz ^{31}P) or 400 MHz ^{1}H (100.6 MHz ^{13}C, 161.7 MHz ^{31}P) or 500 MHz ^{1}H (125.8 MHz ^{13}C) spectrometers in deuterochloroform, chloroform being used as an internal reference. ^{31}P NMR spectra were referenced to external 85% H$_3$PO$_4$ (δ 0.00). Data for NMR spectra are reported as follows: chemical shift in δ, multiplicity abbreviations (br = broad, s = singlet, d = doublet, t = triplet, q = quartet, qu = quintet, m = multiplet), coupling constants reported in Hz(J), integration, and interpretation. In the ^{1}H spectra, unless specified, reported couplings are due to proton–proton coupling. Infrared spectra (IR) were recorded on an IBM FTIR-32 spectrometer. Peaks are reported in units of cm^{-1} with the following relative intensities: s (strong) 100–67% intensity, m (medium) 66–34% intensity, or w (weak) 33–3% intensity. Electron impact (EI) mass spectra were obtained on a Varian MAT-731. Data are reported in the form *m/z* (intensity relative to base = 100). Elemental analyses were performed by the University of Illinois Microanalytical Service Laboratory.

Analytical thin-layer chromatography was performed on Merck silica gel plates with F-254 indicator. Visualization was accomplished by UV light, iodine, or 5% PMA solutions. Solvents for extraction and chromatography were technical grade and distilled from the usual drying agents. The solvents that were used for recrystallization were spectral grade

and are shown after each mp. Column chromatography was performed with 32–63 mm silica gel (Woelm) using the solvents indicated for TLC unless otherwise indicated. Melting points were determined on a Thomas–Hoover capillary melting-point apparatus and are corrected. Bulb-to-bulb distillations were done on a Buchi GKR-50 Kugelrohr: boiling points (bp) refer to air bath temperatures and are uncorrected. All reactions were run under nitrogen.

5,5-Dimethyl-2-phenylmethyl-1,3,2-dioxaphosphorinane 2-Oxide (**7**). Anhydrous triethylamine (1.96 g, 2.7 mL, 19.4 mmol, 5.0 equiv.) and 2,2-dimethyl-1,3-propanediol (404 mg, 3.88 mmol, 1.0 equiv) were dissolved in anhydrous diethyl ether (20 mL) in a flame-dried, 50-mL, three-necked flask equipped with a stir bar, septum, glass stopper, and N$_2$ inlet. The solution was cooled in an ice bath. A solution of benzylphosphonic dichloride [16] (810 mg, 3.88 mmol, 1.0 equiv.) in anhydrous diethyl ether (8 mL) was added rapidly via syringe to the cold diol solution with immediate formation of a white precipitate. The heterogeneous reaction mixture was warmed to ambient temperature and stirred overnight. The triethylamine hydrochloride was removed by filtration and then rinsed with anhydrous diethyl ether (2 × 275 mL). The filtrate was concentrated to give a white solid that was purified by silica gel column chromatography to give 500 mg (54%) of **6**. The solid was further purified by recrystallization in EtOAc/hexane. R_f = 0.41 (hexane/*i*-PrOH, 7/3); mp 108–109°C (EtOAc/hexane); ^{1}H NMR (CDCl$_3$) 7.31 (m, 5 H, phenyl protons), 4.17 (dd, J_{HH} = 11.0, $^3J_{HP}$ = 7.0, 2H, *H*$_2$C–O axial), 3.67 (dd, $^3J_{HP}$ = 15.1 Hz, J_{HH} = 11.2, 2H, *H*$_2$C–O equatorial), 3.28

(d, $^2J_{HP}$ = 21.7 Hz, 2H, P-CH_2-Ph), 0.92 (s, 3 H, CH_3), 0.78 (s, 3H, CH_3); ^{13}C NMR (CDCl$_3$) 134.01 (d, $^2J_{CP}$ = 10.0 Hz, C$_{ipso}$), 129.86 (d, $^3J_{CP}$ = 6.3 Hz, C$_{ortho}$), 128.55 ($^4J_{CP}$ = 2.7, C$_{meta}$), 127.05 ($^5J_{CP}$ = 3.1, C$_{para}$), 75.03 (H$_2$C–O), 32.80 (d, $^1J_{CP}$ = 135.8 Hz, PhCH_2–P), 32.44 [d, $^3J_{CP}$ = 5.6 Hz, (CH$_3$)$_2$-C-(CH$_2$)$_2$], 21.34 (CH$_3$), 21.23 (CH$_3$); ^{31}P NMR (CDCl$_3$) 22.75; IR (KBr) 2961 (m), 2915 (w), 1476 (m), 1455 (w), 1260 (s), 1053 (s), 1009 (s), 980 (m), 858 (m), 816 (m); MS (EI) m/z 240 (M$^+$, 22), 173 (29), 172 (17), 143 (13), 92 (11), 91 (100), 70 (18), 65 (19), 56 (24), 41 (28), 39 (13). Anal. calcd for C$_{12}$H$_{17}$O$_3$P: C, 59.98; H, 7.15; P, 12.89. Found: C, 60.07; H, 7.15; P, 12.97.

5,5-Dimethyl-2-ethyl-1,3,2-dioxaphosphorinane 2-Oxide (**9**). 2,2-Dimethyl-1,3-propanediol (1.92 g, 18.47 mmol) was introduced into a flame-dried 250-mL, three-necked flask equipped with a magnetic stir bar, a rubber septum, and an N$_2$ inlet. Anhydrous triethylamine (12.8 mL, 92.01 mmol, 5.0 equiv.) and diethyl ether (150 mL) were added to the flask. The solution was cooled in an ice bath, and ethylphosphonic dichloride (2.71 g, 18.45 mmol, 1.0 equiv) was added dropwise by syringe. The suspension was warmed to ambient temperature and stirred for 40 hours. The suspension was filtered, and the salts were rinsed with diethyl ether (50 mL). The filtrate was concentrated to give a pale yellow solid. The residue was purified by silica gel chromatography to give 3.18 g (97%) of **9** as a white solid that was recrystallized from hexane to give 2.72 g (83%) of **9** as a white crystalline solid. R_f = 0.68 (EtOAc/i-PrOH, 1/1); mp 107–108°C; ^{1}H NMR (CDCl$_3$) 4.26 (dd, J_{HH} = 10.9, $^3J_{HP}$ = 6.4, 2H, H_2C–O axial), 3.76 (dd, $^3J_{HP}$ = 16.0 Hz, J_{HH} = 11.0, 2H, H_2C–O equatorial), 1.86 (dq, $^3J_{HP}$ = 18.2 Hz, J_{HH} = 7.7, 2H, CH$_3$CH_2–P), 1.23 (dt, $^3J_{HP}$ = 20.3 Hz, J = 7.7 Hz, 3H, CH_3CH$_2$–P), 1.17 (s, 3H, CH_3), 0.96 (s, 3H, CH_3); ^{13}C NMR (CDCl$_3$) 74.17 (d, $^2J_{CP}$ = 6.0 Hz, H$_2$C–O), 32.52 (d, $^3J_{CP}$ = 5.6 Hz, (CH$_3$)$_2$-C-(CH$_2$)$_2$), 21.70 (CH$_3$), 21.20 (CH$_3$), 17.46 (d, $^1J_{CP}$ = 139.5 Hz, CH$_3$CH_2–P), 6.26 (d, $^2J_{CP}$ = 7.4 Hz, CH_3H$_2$C–P); ^{31}P NMR (CDCl$_3$) 31.62; IR (CCl$_4$) 2980 (s), 2946 (s), 2903 (m), 1478 (s), 1458 (m), 1416 (w), 1408 (w), 1366 (m), 1323 (m), 1323 (m), 1269 (s), 1233 (s), 1055 (s), 1036 (s), 976 (s), 953 (s), 922 (s), 833 (s), 812 (s); MS (EI) m/z 178 (M$^+$, 2), 111 (43), 93 (12), 68 (18), 56 (100), 55 (13), 41 (25). Anal. calcd for C$_7$H$_{15}$O$_3$P: C, 47.19; H, 8.49; P, 17.38. Found: C, 47.00; H, 8.45; P, 17.23.

5,5-Dimethyl-2-(1-methylethyl)-1,3,2-dioxaphosphorinane 2-Oxide (**8**). Dioxaphosphorinane **9** (1.05 g, 5.91 mmol) was introduced into a flame-dried, 100 mL three-necked flask equipped with a stirring bar, a low-temperature thermometer, a rubber septum, and an N$_2$ inlet. Anhydrous THF (50 mL) was added to the flask via syringe, and the solution was cooled to an internal temperature of −67°C. Then t-BuLi (1.47 M in pentane, 4.42 mL, 6.5 mmol, 1.1 equiv) was added dropwise via syringe. The yellow solution was stirred at −67°C for 30 minutes, and then iodomethane (1.10 mL, 17.77 mmol, 3.0 equiv) was added all at once via syringe (the solution immediately decolorized). The reaction mixture was stirred at −67°C for 10 minutes, and then the reaction was quenched by adding methanol (5 mL). The solution was warmed to room temperature and the solvent removed by rotary evaporation. NH$_4$Cl solution (50% a*g*, 30 mL) was added, and the aqueous phase was extracted with CH$_2$Cl$_2$ (4 × 40 mL). The combined organic layers were dried (K$_2$CO$_3$), filtered, and concentrated to give a yellow oil. The residue was purified by silica gel chromatography to give 843 mg (80%) of a pale yellow solid that was further purified by Kugelrohr distillation (product sublimed) to give 658 mg (58%) of **8** as a white crystalline solid. R_f = 0.75 (EtOAc-i-PrOH, 1/1); mp 102–103°C; ^{1}H NMR (CDCl$_3$) 4.29 (dd, J_{HH} = 10.9, $^3J_{HP}$ = 4.7, 2H, H_2C–O axial), 3.73 (dd, $^3J_{HP}$ = 17.1 Hz, J_{HH} = 11.0, 2H, H_2C–O equatorial), 2.08 [dheptet, $^3J_{HP}$ = 11.5 Hz, J_{HH} = 7.2 1H, (CH$_3$)$_2$CH–P], 1.26 [dd, $^3J_{HP}$ = 18.7 Hz, J = 7.2 Hz, 6H, (CH_3)$_2$CH–P], 1.19 (s, 3 H, CH_3), 0.92 (s, 3 H, CH_3); ^{13}C NMR (CDCl$_3$) 73.87 (d, $^2J_{CP}$ = 6.0 Hz, H$_2$C–O), 32.70 [d, $^3J_{CP}$ = 4.5 Hz, (CH$_3$)$_2$-C-(CH$_2$)$_2$], 24.63 [d, $^1J_{CP}$ = 138.9 Hz, (CH$_3$)$_2$CH–P], 21.93 (CH$_3$), 21.27 (CH$_3$), 15.74 [d, $^2J_{CP}$ = 4.8 Hz, (CH_3)$_2$CH–P]; ^{31}P NMR (CDCl$_3$) 33.77; IR (CCl$_4$) 2969 (s), 2919 (s), 2874 (m), 1480 (s), 1464 (s), 1406 (m), 1364 (s), 1321 (m), 1302 (s), 1258 (s), 1217 (m), 1059 (s), 1007 (s), 976 (s), 951 (s), 936 (m), 920 (s), 893 (s), 826 (s); MS (EI) m/z 192 (M$^+$, 6), 150 (10), 125 (51), 69 (17), 65 (11), 56 (100), 55 (19), 43 (29), 41 (47), 39 (16). Anal. calcd for C$_8$H$_{17}$O$_3$P: C, 49.95; H, 8.92; P, 16.12. Found: C, 50.15; H, 8.93; P, 16.03.

General Procedure for Variable Temperature NMR Studies. The ^{1}H and ^{13}C NMR spectra were recorded on a General Electric GN-500 spectrometer (^{1}H 500.1 MHz and ^{13}C 125.76 MHz). The ^{31}P, ^{7}Li, and ^{6}Li NMR spectra were obtained on a General Electric GN-300 (34 mm bore, ^{31}P 121. MHz, ^{7}Li 116. MHz, and ^{6}Li 44.23 MHz) or a General Electric GN-500 spectrometer (^{31}P 202.5 MHz, ^{7}Li 194.2 MHz, and ^{6}Li 73.6 MHz). All reported temperatures are calibrated by the method of Van Geet [17]. In all experiments, 5 mm NMR tubes were used, always sealed with a 5 mm septum.

^{1}H NMR spectra were referenced to 3.58 ppm (THF-d_8), and ^{13}C NMR spectra were referenced to 67.40 ppm (quintet, THF-d_8). ^{13}C NMR spectra using dimethyl ether were externally referenced to 67.40 ppm (quintet, THF-d_8). ^{31}P NMR spectra were obtained with proton decoupling and referenced to external 85% H_3PO_4 at room temperature (rt). [6]Li and [7]Li spectra were referenced to 1M LiCl in D_2O at rt. The [6]Li {^{31}P} NMR spectra were obtained on a GN-500 spectrometer using the GE 10 mm [31]P–[15]N broadband probe. [6]Li (73.6 MHz) was observed through the lock channel, while the [31]P (202.5 MHz) was decoupled using the X-Band decoupler through the observe channel (15–20 dB, <1 W CW irradiation).

n-BuLi (10.0 M) was purchased from Aldrich and used as is. THF-d_8 was purchased from Cambridge Isotope Labs and distilled from sodium benzophenone prior to use. Deuterated solvents were used whenever possible to give a stable lock. In all experiments, field homogeneity was achieved by ^{1}H fid shimming (except [7]Li experiments, which used the [7]Li fid). In all reported chemical shifts, the upfield shifts from standard references have negative δ.

General Procedure for X-ray Crystal Structure Determination. Several crystals were removed from the suspension with a small spatula and placed in Paratone-N (Exxon) oil. The crystals were quickly examined (<30 s) under a microscope and then mounted on a thin glass fiber and cooled to $-75°C$. The reflections were observed on an Enraf-Nonius CAD-4 automated κ-axis diffractometer equipped with a graphite crystal monochromator. Variable scan rates from 3 to 16°/min were used.

X-ray Crystal Structure of Lithio-5,5-Dimethyl-2-isopropyl-1,3,2-dioxaphosphorinane 2-Oxide (Li^+8^-). 5,5 Dimethyl-2-isopropyl-1,3,2-dioxaphosphorinane 2-oxide (**8**) (10.0 mg, 0.05 mmol) was introduced into a flame-dried test tube (5 × 50 mm) fitted with a rubber septum and a N_2 inlet (syringe needle). Anhydrous TMEDA (170 μL) and THF (9 μL) were added via syringe, and the resulting solution was cooled in an ice bath. *n*-BuLi (7.9 M in hexane, 10 μL, 0.08 mmol, 1.5 equiv) was added dropwise via syringe (final concentration 0.28 M). The colorless solution was stored in a freezer ($\approx -20°C$). Clear, colorless crystals formed over a 12–16 hour period. The crystal used in the X-ray analysis was mounted directly from the supernatant solution.

REFERENCES

[1] (a) L. Horner, H. Hoffmann, H. G. Wippel, *Chem. Ber., 91,* 1958, 61; (b) W. S. Wadsworth, W. D. Emmons, *J. Am. Chem. Soc., 83,* 1961, 1733; (c) W. S. Wadsworth Jr., *Org. React., 25,* 1977, 73; (d) B. J. Walker: in J. I. G. Cadogan (ed): *Organophosphorus Reagents in Organic Synthesis,* Academic Press, New York, chap. 3 (1979); (e) S. E. Kelly: in S. L. Schreiber (ed): *Comprehensive Organic Synthesis, Additions to C-X π Bonds, Part 1,* Pergamon Press, Oxford, vol 1, chap. 3.1 (1991) and references cited therein.

[2] S. E. Denmark, C.-T. Chen, R. A. Read, *Advances in Carbanion Chemistry,* submitted.

[3] (a) S. E. Denmark, R. L. Dorow, *J. Am. Chem. Soc., 112,* 1990, 864; (b) S. E. Denmark, P. C. Miller, S. R. Wilson, *J. Am. Chem. Soc., 113,* 1991, 1468; (c) C. J. Cramer, S. E. Denmark, P. C. Miller, R. L. Dorow, K. A. Swiss, S. R. Wilson, *J. Am. Chem. Soc., 116,* 1994, 2437.

[4] (a) S. E. Denmark, K. A. Swiss, S. R. Wilson, *J. Am. Chem. Soc., 115,* 1993, 3826; (b) S. E. Denmark, K. A. Swiss, *J. Am. Chem. Soc., 115,* 1993, 12195; (c) M. Kranz, S. E. Denmark, K. A. Swiss, S. R. Wilson, *J. Org. Chem., 61,* 1996, 8551.

[5] S. E. Denmark, K. A. Swiss, S. R. Wilson, *Angew. Chem., Int. Ed. Engl., 35,* 1996, 2515.

[6] F. A. Cotton, R. A. Schunn, *J. Am. Chem. Soc., 85,* 1963, 2394.

[7] (a) M. Kirilov, P. Petrov, *Chem. Ber., 104,* 1971, 3073; (b) M. Kirilov, G. Petrov, *Monatsh. Chem., 103,* 1972, 1651; (c) G. Petrov, I. Velinov, M. Kirilov, *Monatsh. Chem., 104,* 1973, 1301; (d) E. Weiss, J. Kopf, T. Gardein, S. Corbelin, U. Schümann, M. Kirilov, G. Petrov, *Chem. Ber., 118,* 1985, 3529; (e) J. Macicek, O. Angelova, G. Petrov, M. Kirilov, *Acta Cryst. C, 44,* 1988, 626; (f) O. Angelova, E. Kirilov, M. Kirilov, G. Petrov, J. Kaneti, J. Macicek, *J. Chem. Soc. Perkin Trans., 2,* 1989, 1405.

[8] For a compilation ^{31}P NMR shifts of β-keto and other phosphonate structures, see (a) J. Seyden-Penne, M.-P. Simmonin, T. Strzalko: in J. C. Tebby, (ed): *CRC Handbook of Phosphorus-31 Nuclear Magnetic Resonance Data,* CRC, Boca Raton, FL, pp. 495–500 (1991); (b) review: J. Seyden-Penne, *Bull. Soc. Chim. Fr.,* 1988, 238 and referenced cited; (c) for a brief review of older work, see J. Corset, *Pure Appl. Chem., 58,* 1986, 1133.

[9] (a) M.-P. Teulade, P. Savignac, E. E. Aboujaoude, N. Collignon, *J. Organomet. Chem., 287,* 1985, 145; (b) M.-P. Teulade, P. Savignac, E. E. Aboujaoude, N. Collignon, *J. Organomet. Chem., 312,* 1986, 283; (c) P. Savignac, M.-P. Teulade, N. Collignon, *J. Organomet. Chem., 323,* 1987, 135; (d) M.-P. Teulade, P. Savignac, E. About-Jaudet, N. Collignon, *Phosphorus Sulfur, 40,* 1988, 105; (e) P. Savignac, M.-P. Teulade, C. Patois,

Phosphorus, Sulfur and Silicon, 49/50, 1990, 169; (f) C. Patois, P. Savignac, *Tetrahedron Lett.,* 1991, 1317.

[10] (a) C. Yuan, J. Yao, S. Li, Y. Ma, X. Zhong, *Phosphorus, Sulfur and Silicon, 46,* 1989, 25; (b) C. Yuan, J. Yao, S. Li, *Phosphorus, Sulfur and Silicon, 55,* 1991, 125.

[11] (a) For a review, see S. Bradamante, G. A. Pagani: V. Snieckus, (ed): *Advances in Carbanion Chemistry,* JAI Press, Greenwich, vol. 2, pp. 189–263 (1996); (b) for substituent effects on substituted *P*-benzylphosphonates, see S. Smith, H. Zimmer, E. Fluck, P. Fischer, *Phosphorus Sulfur, 30,* 1987, 327.

[12] W. Zarges, M. Marsch, K. Harms, F. Haller, Frenking, G. Boche, *Chem. Ber., 124,* 1991, 861.

[13] For a manganese complex, see (a) M. G. Newton, N. S. Pantaleo, R. B. King, S. P. Diefenbach, *J. Chem. Soc., Chem. Commun.,* 1979, 55; for platinum complexes, see (b) I. J. B. Lin, L. T. C. Kao, F. J. Wu, G. H. Lee, Y. Wang, *J. Organomet. Chem., 309,* 1986, 225; for mercury complexes, see (c) D. Seyferth, R. S. Marmor, *J. Organomet. Chem., 59,* 1973, 231; (d) S. M. Bowen, E. N. Duesler, R. T. Paine, C. F. Campana, *Inorg. Chim. Acta, 59,* 1982, 53.

[14] This structure is also quite different from the solid-state structure of lithio isopropyl phenyl sulfone. This compound does not display a C–Li contact but does dimerize in a sulfone bridged eight-membered ring. H.-J. Gais, J. Vollhardt, G. Hellman, H. Paulus, H. J. Lindner *Tetrahedron Lett., 29,* 1988, 1259.

[15] For a critical review on the facts of organolithium complexation by TMEDA, see D. B. Collum, *Accounts Chem. Res., 25,* 448.

[16] Benzylphosphonic dichloride was prepared by the method of T. Morita, Y. Okamoto, H. Sakurai, *Chem. Lett.,* 1980, 435, and R. S. Rogers, *Tetrahedron Lett.,* 1992, 7473.

[17] A. L. Van Geet, *Anal. Chem., 40,* 1968, 2227.